ADVANCED HEALTHCARE MATERIALS
www.advhealthmat.de



# Ultrathin and Robust Hydrogel Coatings on Cardiovascular Medical Devices to Mitigate Thromboembolic and Infectious Complications

*German Parada, Yan Yu, William Riley, Sarah Lojovich, Diane Tshikudi, Qing Ling, Yefang Zhang, Jiaxin Wang, Lei Ling, Yueying Yang, Seemantini Nadkarni, Christoph Nabzdyk,* and Xuanhe Zhao**

**Thromboembolic and infectious complications stemming from the use of cardiovascular medical devices are still common and result in significant morbidity and mortality. There is no strategy to date that effectively addresses both challenges at the same time. Various surface modification strategies (e.g., silver, heparin, and liquid-impregnated surfaces) are proposed yet each has several limitations and shortcomings. Here, it is shown that the incorporation of an ultrathin and mechanically robust hydrogel layer reduces bacterial adhesion to medical-grade tubing by 95%. It is additionally demonstrated, through a combination of in vitro and in vivo tests, that the hydrogel layer significantly reduces the formation and adhesion of blood clots to the tubing without affecting the blood's intrinsic clotting ability. The adhesion of clots to the tubing walls is reduced by over 90% (in vitro model), which results in an ≈60% increase in the device occlusion time (time before closure due to clot formation) in an in vivo porcine model. The advantageous properties of this passive coating make it a promising surface material candidate for medical devices interfacing with blood.**

Cardiovascular devices such as intravascular (IV) catheters are essential for the diagnosis and treatment of many acute and chronic diseases (including cancer, end-stage renal disease, cardiovascular disease, etc.), including the care for critically ill patients in the ICU.[1–10] The US market for these medical devices in 2016 was ≈$9.0 billion with an expected growth rate of 4.7% due to the higher incidence of chronic diseases and an overall aging, frailer population.[11,12] Given their widespread use, serious complications such as infections (5–15% rate)[4,8,13] and thrombosis (10–20% rate)[8,14] are always of concern to clinicians, as they can lead to life-threatening complications such as sepsis, pulmonary embolism and deep-vein thrombosis. These two complications are commonly seen when using indwelling IV catheters such as central venous catheters (CVCs), hemodialysis catheters, and peripherally inserted central catheters (PICCs), as those are often used for longer durations (weeks to months).[1,2,4,5,8,14–16] Moreover, catheter-related complications are costly and challenging to treat as the patients that depend on these catheters are likely frail and/or acutely ill (e.g., in the ICU, patients with severe infections, cancer). Aside from the increased

Dr. G. Parada
Chemical Engineering Department
Massachusetts Institute of Technology
Cambridge, MA 02139, USA

Dr. G. Parada, Dr. Y. Yu, Y. Yang, Prof. X. Zhao
Mechanical Engineering Department
Massachusetts Institute of Technology
Cambridge, MA 02139, USA
E-mail: zhaox@mit.edu

Dr. Y. Yu, Y. Yang
School of Optical and Electronic Information
Huazhong University of Science and Technology
Wuhan, Hubei 430064, China

W. Riley, S. Lojovich
Perfusion Services
Massachusetts General Hospital
Boston, MA 02114, USA

D. Tshikudi, Prof. S. Nadkarni
Wellman Center for Photomedicine
Massachusetts General Hospital
Boston, MA 02114, USA

Dr. Q. Ling, Dr. Y. Zhang, Dr. J. Wang, Dr. L. Ling
Tongji Medical School
Huazhong University of Science and Technology
Wuhan, Hubei 430064, China

Prof. C. Nabzdyk
Department of Anesthesia
Critical Care and Pain Medicine
Massachusetts General Hospital
Boston, MA 02114, USA
E-mail: Nabzdyk.Christoph@mayo.edu

Prof. C. Nabzdyk
Department of Anesthesiology and Perioperative Medicine
Mayo Clinic Rochester
Rochester, MN 55902, USA

The ORCID identification number(s) for the author(s) of this article can be found under https://doi.org/10.1002/adhm.202001116

**DOI: 10.1002/adhm.202001116**

morbidity and mortality associated with, e.g., central venous and urinary catheters, these complications and the associated care costs pose a significant burden on the health care system as a whole.

These complications are not unique to catheter devices, as they have also been reported for other blood-contacting devices such as stents, prosthetic bypass grafts, dialysis equipment, ventricular-assisted devices (VADs), artificial heart valves, and extracorporeal membrane oxygenation (ECMO) equipment.[17–22] Despite significant efforts, infectious and thromboembolic complications associated with the use of cardiovascular medical devices continue to represent a significant, unmet clinical challenge, especially given the increasing population of chronically ill patients that depend on these devices.

There are currently no commercially available solutions that sufficiently address both thrombosis and infection complications. Most of the commercially available technologies target infectious complications. Those approaches include antiseptic wound dressings, antibiotic-coated catheters and antibiotic-impregnated catheters.[7,13,23–28] These technologies show modest reduction of bacteremia but only for select patient populations and short-term catheter usage. None of these approaches yields a device surface that intrinsically decreases bacterial adhesion and thereby mitigates bacterial biofilm formation. Moreover, there is no improvement pertaining to other side effects of catheter usage (including thrombosis), and no proven clinical benefit for long-term applications.[23,24] A separate set of available technologies aims to address thrombosis and the subsequent device occlusion. These approaches rely on attaching bioinert polymers or bioactive molecules such as corn trypsin inhibitor, heparin or thrombomodulin, to the device surface.[6,10,29–32] Despite promising preclinical data, the clinical trial performance has been mixed—only select heparin-coating technologies are able to show clinical benefits.[3,5,6,30]

There are very few technologies that aim to address both thrombosis and infections. One approach involves the incorporation of a nanotextured surface that is entrained with perfluorinated liquids.[33–35] This surface repels both bacteria and blood components, however, it has not been translated to clinical use likely due to concerns about the presence of fluorine-containing fluids in bloodstream. A second approach involves the photografting of hydrophilic polymers onto the device surface.[7,36–40] This is a mature technology that was initially developed in the 1980s to reduce the friction and irritation for urinary catheters, and was marketed as a "hydrogel-coating" technology even though it only involves surface polymer grafting and not a 3D polymer network. Most major brands now offer "hydrogel-coated" catheters, with brand names such as Biocath and Lubri-sil (Bard), Flocath (Teleflex), Serpia (Braun), Convey and HydroPlus (Boston Scientific), and HydroPicc (Access Vascular).[41–43] Despite showing clinical performance and being adopted by healthcare professionals, there are concerns about adverse effects stemming from coating failure and delamination, since these grafted coatings are usually tens of nanometers thick.[41,42] The evidence led the FDA to issue a safety communication in 2015 and a labeling guidance in 2019 to address these complications.[44,45] Based on the current clinical data and published literature it is evident that the development of a thrombosis-resistant and bacteria-repellent surface would be a major advancement in the ever growing field of cardiovascular and critical care devices.

In this study, we have characterized the mechanical, antibacterial, and thrombosis-resistant properties of ultrathin hydrogel layers introduced on medical device surfaces. The robust adhesion of tough hydrogel materials, a technology recently developed by our group,[46–48] showed the potential to enhance the interfacial properties of elastomer-based medical interfaces. In the experiments discussed here we have used medical-grade Tygon (polyvinyl chloride) tubing, a standard medical device used for blood management in dialysis and cardiopulmonary bypass settings.[12,19] This was done to ensure the blood only contacts a single material, as the blood would be fully contained inside the tubing. Any tests conducted with catheters would require an outer vessel (of a different material) to contain the blood, which is undesired as it may have complicated the analysis. The coated surfaces had low coefficients of friction and withstood fluid flow at physiological rates up to 12 h without any measurable changes. The adhesion of bacteria and fibrin is significantly reduced in comparison to uncoated surfaces. In addition, through a series of in vitro assays and flow loop tests, we showed that the hydrogel coating decreased the formation and adhesion of blood clots to the device surface without compromising the blood's innate clotting ability. Moreover, we demonstrated in pigs the superior patency rates of hydrogel-coated PVC tubings that were implanted into the systemic circulation (arterial to arterial connection). These initial results indicate that hydrogel coatings of blood-contacting devices may mitigate infection and thrombosis-related complications of cardiovascular devices and thus could obviate technologies aimed to address these clinical problems individually.

The hydrogel coatings were prepared as previously described.[48] This method was chosen as it allowed for the coating of flat surfaces and of the inner and/or outer surface of cylindrical devices (e.g., catheters and tubing). Following published protocols, the coatings in this work were created by first submerging the clean medical surfaces in a benzophenone solution in ethanol. The solution was removed and then an aqueous pregel solution containing *N,N*-dimethylacrylamide (DMAA) and a biocompatible photoinitiator (Irgacure 2595) was added on the activated surfaces. This monomer was chosen to avoid the toxicity concerns of using acrylamide, the monomer used in previous publications.[49] The surface was then irradiated with UV to polymerize the hydrogel layer. After thorough rinsing of the excess polymers and byproducts, the result was an ultrathin (≈10 µm) hydrogel layer uniformly coated on the device, as shown schematically in **Figure 1**a for Tygon CPB tubing. The layer is very thin compared to the typical OD of venous catheters (5–6 mm) or the ID of blood-management tubing (0.75–1.5 cm). Macro images of pristine and coated (inner lumen only) tubing are shown in Figure 1b to demonstrate that the hydrogel coating was uniform and did not affect the overall device dimensions due to its micrometer-sized dimensions. Microscopy images of the cross-section are shown in Figure S1 (Supporting Information). Further details on the chemical composition of the hydrogel coating, the fabrication process and the adhesion mechanism can be found in a previous publication.[48]

The elastic modulus of the hydrogel layer was determined previously to be $E \approx 30$ kPa ,[48] value which is two orders of

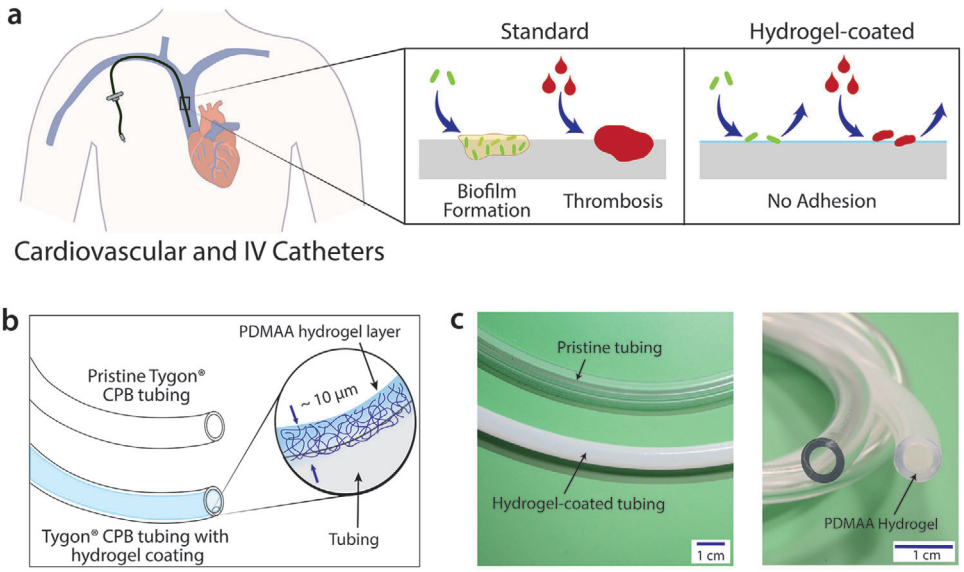


**Figure 1.** Hydrogel coatings on medical device surfaces. a) Schematic illustration of the mitigation of bacterial adhesion and thrombosis on vascular medical devices through the use of the proposed ultrathin hydrogel coatings. b) The medical device used in this study is Tygon cardiopulmonary bypass (CPB) tubing, both pristine and hydrogel-coated. The hydrogel coating is shown schematically here highlighting its micrometer-sized thickness. c) Macroscopic images of coated and pristine tubing to demonstrate the methodology used here generates even and uniform hydrogel coatings on feet-long tubing segments.

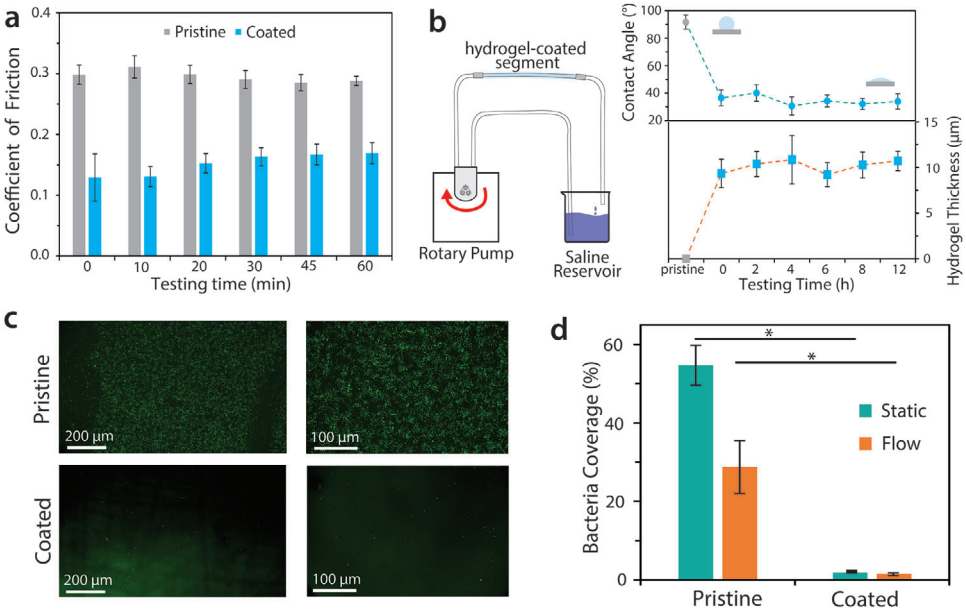


**Figure 2.** Mechanical and antibacterial properties of hydrogel-coated surfaces. a) Coefficient of friction (COF) of pristine and coated surfaces continuously sheared for 1 h. Error bars represent SD of the COF values time-averaged over 3 min. b) Contact angle and hydrogel layer thickness measurements after continuous flow of saline solution (flowrate ≈ 1.5 L $min^{-1}$) for up to 12 h in the apparatus depicted to the left. Error bars represent SD of multiple measurements for each time point. c) Representative fluorescent microscopy images of pristine and coated surfaces with GFP-expressing *E. coli* in bright green. d) Quantification of *E. coli* (area) coverage of pristine and coated surfaces for static and flow testing conditions. The flow condition was carried out in an apparatus similar to that shown in subsection (b). Error bars represent SD of multiple areas analyzed.

magnitude lower than the pristine Tygon substrate ($E \approx 6$ MPa). The presence of the water-containing hydrogel layer decreased the coefficient of friction (COF) of the surface,[50–53] tested here using a rheometer with a steel parallel plate geometry, as described previously.[47,48] We characterized the COF of both pristine and coated flat surfaces with continuous shearing with a normal force of 1 N up to 60 min, as shown in **Figure 2**a. The COF of the coated surface was consistently lower than that of the pristine surface throughout the experiment (0.1–0.15 vs 0.30), demonstrating the remarkable mechanical robustness of the

interpenetrated hydrogel layer. Coatings with are not robust would have been eroded by the constant shearing and the COF would increase to a similar value as the uncoated substrate. It is important to note that these loading conditions exceeded those eventually seen in actual applications. The coating could also withstand fluid flow at physiologically relevant rates (≈1.5 L $min^{-1}$) and pressures (≈100 mmHg). Using the setup shown in Figure 2b, saline was circulated continuously for up to 12 h through a coated tubing segment. At selected time points, the surface water contact angle was measured by the sessile drop method, and the coating thickness was assessed using fluorescent microscopy. Since the pristine Tygon surface is hydrophobic, the measured contact angle of the pristine sample was above 80°. A decrease in the measured contact angle (under 40°) was observed after the introduction of the ≈10 µm hydrogel coating. There was no change in the contact angle or coating thickness after continuous flow up to 12 h, evidence of the robustness and integrity of the hydrogel coating.

Previous publications have shown that hydrated surfaces (grafted polymers and bulk hydrogels) can serve as antifouling layers to prevent the adhesion of unwanted agents.[7,39,47,48,54] The antifouling performance of the DMAA-based ultrathin hydrogel coatings was assessed with regards to their in vitro efficacy against bacterial and fibrin adhesion. Coated and pristine surfaces were contacted with media containing engineered *Escherichia coli* and incubated for 4 and 8 h in static and flow conditions, respectively. *E. coli* is a common pathogen seen in ambulatory and nosocomial infections,[2,4,7,8] and the strain used in these experiments was engineered to express GFP for easy visualization using fluorescent microscopy. Bacterial adhesion and colonization of coated surfaces were significantly reduced in both static and flat tests as compared to the pristine surfaces ($p << 0.05$), as shown in Figure 2c. Microscope imaging as shown in Figure 2d revealed that the hydrogel coating prevented bacterial adhesion even in the absence of eluting antibiotics.

In a similar fashion, coated and pristine surfaces were incubated with heparinized human blood containing Alexa Fluor 488-tagged fibrinogen, following published protocols.[34,35] This allowed for visualization of the fibrin network formation as the blood started to coagulate on the surfaces. As shown in **Figure 3**a, confocal microscopy imaging revealed that fibrin deposition and network formation was significantly greater on the pristine substrates for every time point as compared to the coated ones. It is important to note that no macroscopic clotting was seen in these experiments as the blood was heparinized. The quantification across various representative areas and samples is shown in Figure 3b, and was comparable with the antifouling behavior reported for hydrogels and perfluorinated surfaces.[34–37,54] A similar adhesion-resistant behavior against other blood proteins and factors in the coagulation cascade is expected for the hydrogel coatings presented in this work, although additional work would be needed to verify and quantify this hypothesis.

Next, bovine whole blood was used to further characterize the interaction of surface coating and blood in a setting closer to the intended applications than the tests described above. The objective of the following tests was to compare device-related thrombus formation, adhesion, and occlusion for coated and uncoated tubing, tests required under the ISO standard to evaluate the blood compatibility of medical devices.[55] Bovine blood was chosen since it is commercially available and large blood volumes (>50 mL) were needed for these experiments. As stasis promotes coagulation,[3,15,16,32,56] experiments were conducted while maintaining constant motion of the blood phase in order to minimize this confounder and to characterize the interaction of blood and surface coating more exclusively.

The first test was a simple approach to introduce flow, and this was done by moving a column of blood back and forth inside tubing until clotting occurred, as shown in the videos in the Supporting Information. The occlusion time was defined as the time when a macroscopic thrombus occluded the lumen of the tube and thus no blood movement could be seen when inverting the tubing. The results of several tests carried out are shown in Figure 3c. In the absence of movement (i.e., stasis), the clotting time for coated and pristine tubes was no different than that of the control (blood in an Eppendorf tube). When the blood was agitated, the measured clotting time was longer in coated tubing than in pristine tubing. The spread in the data most likely represented variability in the blood samples used, as the tests were run at different days. In addition, it is important to notice that the 5 topmost coated tests were arbitrarily stopped at $t = 25$ min even though blow flow within the tubing was still observed. Upon closer inspection there was still uncoagulated blood inside the tubing, and the thrombi noted were not attached to the tubing surface unlike in the pristine tubing tests.

Overall these were very promising results suggesting that the coating had the potential to improve the performance of blood-contacting devices passively, i.e., without the presence of an anticoagulant such as heparin or citrate. While the use of heparin-containing surfaces has been proposed to reduce thrombosis complications (such as GORE CARMEDA or Medtronic Cortiva bioactive coatings), the introduction of heparin also carries negative side effects such as the risk of hemorrhage and heparin-induced thrombocytopenia. Moreover, this local anticoagulant property is difficult to control and may have unpredictable effects in patients with abnormal coagulation. Overall the clinical effect of these heparin-coated surfaces is modest and short-lived at best.

One potential explanation for the results seen in Figure 3c could have been that the hydrogel coating interferes with the blood's coagulation cascade by either cell lysis, binding or denaturing of key factors. Thus, two experiments were carried out to rule out these scenarios. First, whole blood samples were incubated on top of pristine and coated tubing under mild agitation and subsequently collected and pelleted using a centrifuge. The supernatant was analyzed with a spectrophotometer at the strongest absorption frequencies for oxygenated hemoglobin (540 and 576 nm).[57] The samples were compared to a negative control (untreated bovine blood) and a hemolyzed positive control (hypotonic hemolysis), as shown in Figure 3d. The measurements confirmed that the coating did not cause any significant hemolysis when compared to the negative control (baseline). Hemolysis would have resulted in the release of hemoglobin from the red blood cell cytoplasm into the supernatant, which would have resulted in higher absorbance values.

Second, optical thromboelastography (OTEG) was performed to quantify the effect of the hydrogel coating on the blood clotting process.[58–60] This method, illustrated schematically in Figure 3e, analyzes the autocorrelation function of a reflected laser beam and generates an OTEG graph (shown at the bottom of

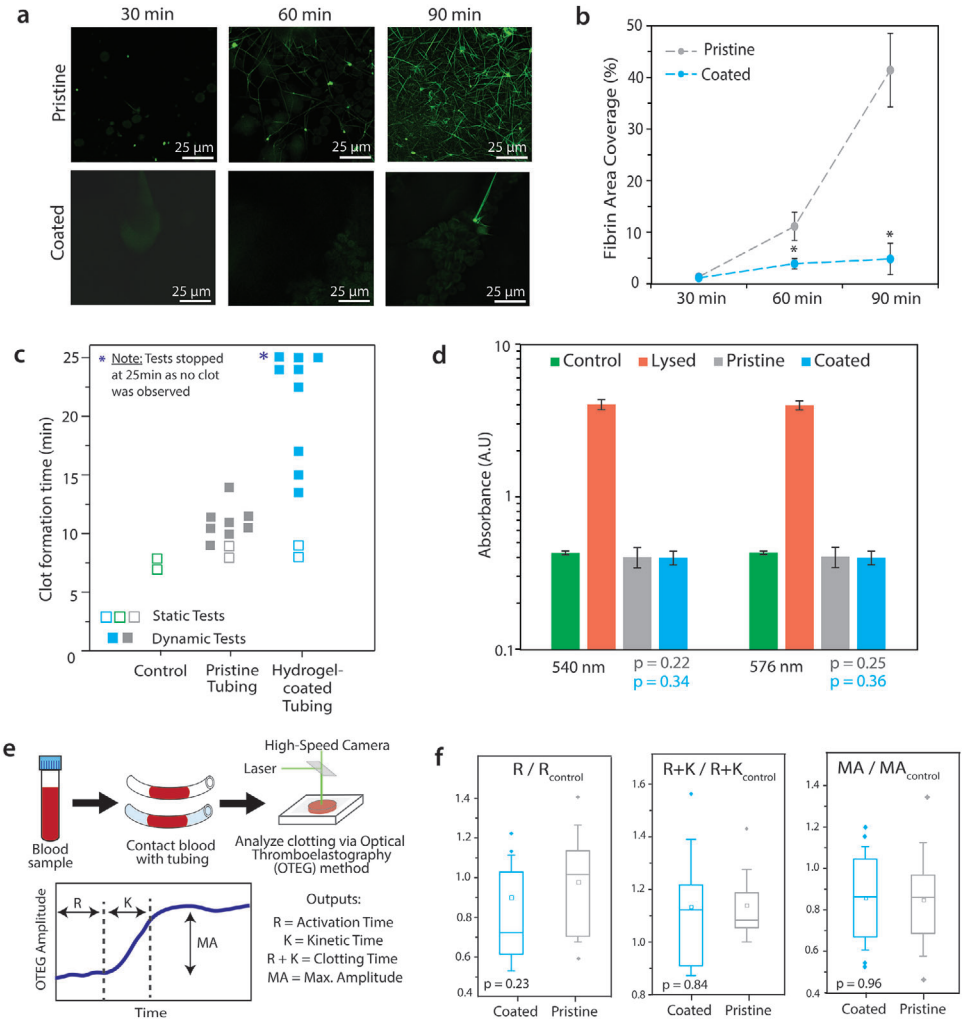


**Figure 3.** In vitro dynamic and static blood tests. a) Representative images of fibrin network formation on pristine and coated surfaces. Fluorescently tagged fibrinogen was added to blood for visualization of the network. b) Area coverage of fibrin network on surfaces. Error bars represent SD of multiple areas analyzed. c) Time elapsed until the tubing was occluded by clot formation for pristine and coated tubing under static or dynamic (agitation) conditions. Control used was an Eppendorf tube. d) Absorbance of the supernatant after centrifugation of blood in contact with pristine and coated tubing at the main wavelengths for oxygenated hemoglobin. Controls used were as-received blood, and lysed blood. Error bars represent SD of 3–4 samples. e) Schematic of modified optical thromboelastography (OTEG) experiments and parameters quantified. f) Box plots of normalized activation time ($R$), clotting time ($R + K$), and max. amplitude (MA) of blood in contact with coated and pristine tubing. The normalization was done with a control sample (analyzed without contact with tubing) to account for variability in blood samples.

Figure 3e).[58] The rising curve indicates the clotting of the blood, where $R$ is the activation time (time until clotting starts) and $R + K$ is the total clotting time. The strength of the clot is measured by the MA (max. amplitude) value. We compared the clotting times and clot strength of blood samples that were placed in pristine and coated tubes as shown in Figure 3e,f. The values were normalized by those of a control sample (blood left in Eppendorf vial) to account for sample variability, and the data is presented as whisker plots. Both $R$, $R + K$ and MA values of pristine and coated tubes were not different from each other (as indicated by $p$-values above 0.05 from $t$-tests), indicating that the hydrogel coating does not interfere with coagulation itself (unlike heparin-eluting or heparin-coated surface) and that stasis must be avoided in order to highlight the beneficial effects of the hydrogel coating.

In a separate, clinically relevant in vitro experiment simulating a cardiopulmonary bypass (CPB) circuit, closed circular tube loops (Tygon CPB tubing) were created and whole blood was circulated through the loops using a CPB machine roller pump (**Figure 4**a). In this scaled-down model of a CBP circuit used during cardiac surgery, low flow rates of 0.25 L min$^{-1}$ were used to avoid over-pressurization, leakage from the circuit, and hemolysis. The blood in the loops was circulated until a control blood sample (in stasis in an Eppendorf vial) fully coagulated. The contents were poured into a petri dish and the clot was removed and weighed. The tubing was gently rinsed twice with saline and then weighted. Bovine blood that was circulated through pristine tubing formed larger amounts of wall-adhering clots than blood in contact with coated tubing, as shown in Figure 4b. The quantitative results from three repeat experiments is shown in Figure 4c.

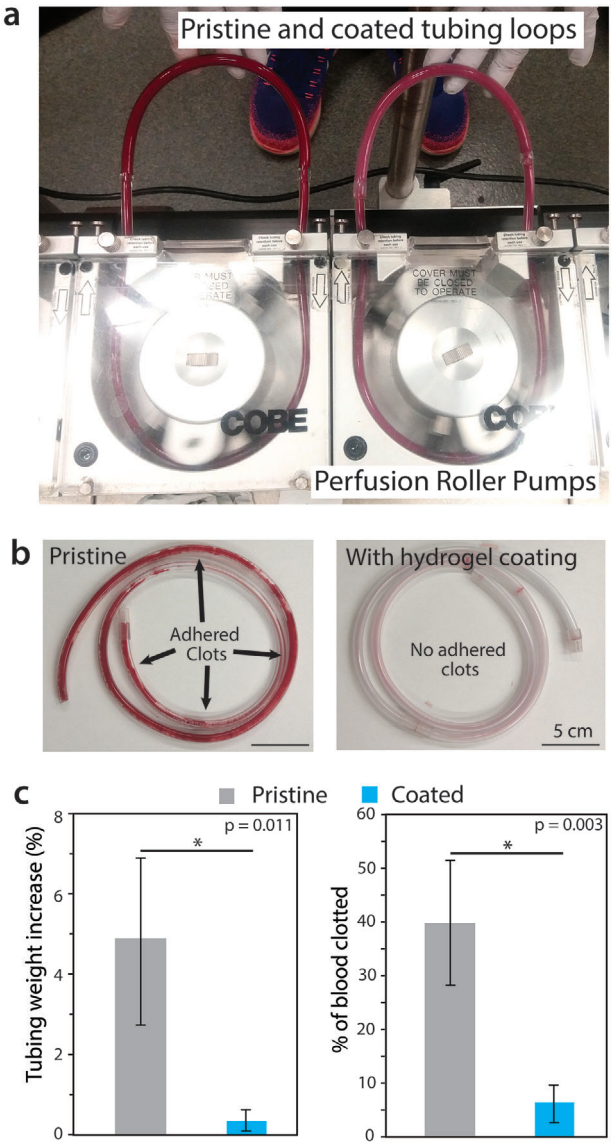


**Figure 4.** In vitro blood loop tests. a) Image of apparatus used for continuous flow testing of pristine and coated tubing. Testing was done in parallel to accurately control the end time point of flow. b) Image of pristine (left) and coated (right) tubing after flow testing and gentle rinsing with saline. c) Quantification of blood clotting and clot adhesion to the tubing walls for blood flow experiments. Error bars represent SD for three repeated experiments.

The mean tubing weight increase for the pristine tubing is 5.03% while that of coated tubing is 0.19%. This statistically significant increase ($p < 0.05$) indicates that blood clots adhered more readily to the pristine than to the coated tubing. Next, the fraction of the original blood that had formed a blood clot was assessed (clots adhered to the tubing and those in the petri dish). Approximately 40% of the blood in contact with the pristine tubing clotted, as compared to the 6.2% of that in contact with the coated tubing. This difference is also significant with p = 0.003.

These two results are very promising evidence that the hydrogel coatings on Tygon tubing and other elastomer-based blood contacting devices show potential to address thrombosis-related complications without the need of heparin or other antithrombosis medications. It is conceivable that the hydrated, lubricious surface of the coated tubing decreased the adhesion and/or activation of either platelets or coagulation factors, as suggested by previous publications.[9,10,56,44] Additional work is required to fully understand the mechanisms behind the beneficial effects mediated by these hydrogel coatings, and to tailor the hydrogel chemistry and fabrication methods to further improve their performance.

To further demonstrate that the developed hydrogel coating can delay clotting on medical devices in the absence of anticoagulation medication, we carried out a small preliminary in vivo study in which tubing was used as an arterial bypass on the iliac artery of anesthetized Bama pigs. No anticoagulation medicine such as heparin was administered. A schematic is shown in **Figure 5**a. Briefly, an incision was made on the groin area and an ≈7 cm section of the iliac artery was exposed. The two ends were clamped with a hemostat and small incisions were made at about 1 cm distal to the clamping. The bypass device was inserted into the incisions and sutured to avoid leakage. The clamps were then released and Doppler ultrasound and ultrasound imaging was used to measure the flow of blood through the bypass and thrombus formation inside the bypass (Figure 5c,d). The experiment was stopped when no more blood flow was observed from the ultrasound imaging, and the occlusion time was recorded.

Uncoated and hydrogel-coated medical-grade silicone tubing (1.2 mm ID, 7 cm length) were sterilized and used as the arterial bypass in this preliminary study. Silicone tubing was used as it is more flexible and has smaller wall thickness than the Tygon tubing used in previous sections. Three experiments were run for each condition. For the uncoated devices, the mean occlusion time was 366.7 s with an SD of 90.7 s, as shown in Figure 5e. The mean occlusion time for the hydrogel-coated devices was 590.5 s with an SD of 130.9 s, time that was longer than that of the uncoated device ($p = 0.032$ from one-tail $t$-test). In the absence of systemic anticoagulation, introducing a hydrogel coating to the devices resulted in a 60% increase in the occlusion time. The result of this preliminary in vivo experiment matches the result obtained in the in vitro experiment, supporting our earlier findings that introducing an ultrathin hydrogel coating on elastomer-based medical devices can delay the formation and adhesion of blood clots to the device surfaces. It is important to note that this result was obtained with a different (and more realistic) blood flow pattern and with narrower lumen dimensions, which suggests the geometry of the device is not relevant as long as the blood-contacting surface has a uniform and thin hydrogel coating. In particular, the variables in this experiment (e.g., arterial bypass instead of arterial to venous fistula and very small inner luminal diameter) were purposely chosen to worsen the flow profile through the tubing and thereby rapidly precipitate vascular occlusion. Therefore, these significant differences in patency are very encouraging.

We conclude that the present study could serve as an early proof-of-concept for using the hydrogel-coating technology as a design strategy that may mitigate the thromboembolic and infectious complications that arise from the use of blood-contacting medical devices.

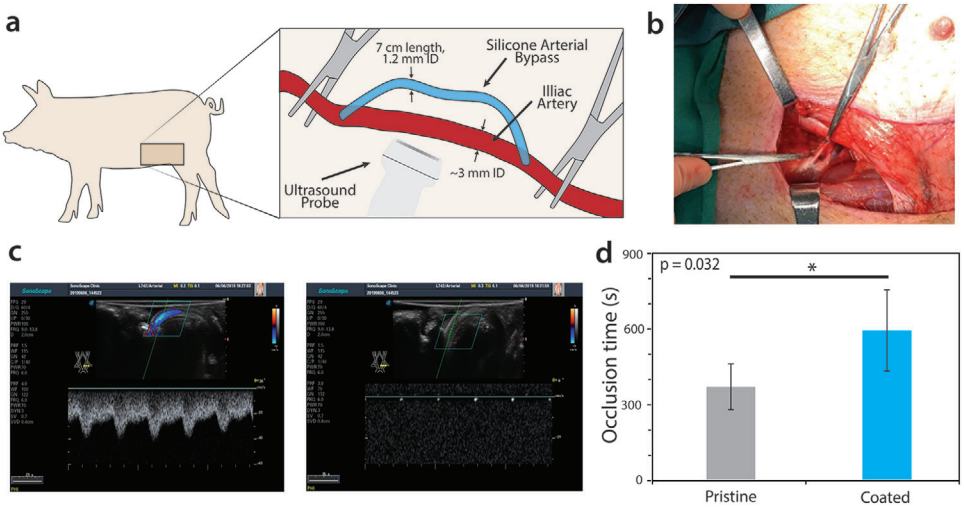


**Figure 5.** In vivo device occlusion tests. a) Schematic of porcine model used to assess the performance of the coated devices under constant blood flow. b) Image of iliac artery to which the silicone tubing was attached to. The incision allowed access for direct ultrasound-based flow monitoring within the silicone tubing. c) Doppler ultrasound images of the devices at the start of the experiment (left) and at the end of the experiment (right). The absence of blood flow velocities on ultrasound measurements indicated that the device is occluded by a clot attached to its inner surface. d) Quantification of the occlusion time of the devices in three repeated experiments. Error bars represent the SD for three repeated experiments.

## Experimental Section

*Hydrogel Coatings on Tygon Surfaces*: All chemicals were purchased from Millipore-Sigma and used as received, unless indicated otherwise. The experimental protocol was as follows. The medical-grade (U.S. Plastic Corp.) flat surface or tubing was cut to the desired size, cleaned with isopropanol and DI water, and fully dried with a nitrogen stream. The devices are then air-plasma treated (PDC-001, Harrick Plasma, <350 torr, 18 W) for 1–2 min and submerged in a benzophenone solution (10 wt% in ethanol) for 3–5 min. The devices are removed from the solution, the excess ethanol is removed by blotting with tissue, and the devices are submerged in a previously degassed hydrogel precursor solution (20–30 wt% *N*,*N*-dimethylacrylamide, 0.5 wt% Irgacure I-2959 in water). For flat surfaces, there should be at least 5 mm of precursor solution above the surface. For tubing, the precursor solution should completely fill the inner lumen. The devices were then exposed to UV (UVP CL-1000, $\lambda = 365$ nm) for 45 min to create the interpenetrating hydrogel layer on the device surface. The polymerized solution was removed and disposed as waste. The devices were thoroughly washed with DI water for 3 days (submerged in water and left in the shaker for flat surfaces, connected to a peristaltic CBP (VWR, variable flow pump) for tubing) before testing.

*Friction Measurements*: The Coefficient of Friction was measured for flat surfaces (5 × 5 cm) using a rheometer (AR-G2, TA Instruments) in normal force control mode with a 20 mm steel parallel plate geometry. The coefficient of friction was calculated from the measured torque and normal force following a protocol used previously.[39,40] Briefly, pristine and coated samples were loaded into the rheometer and a 1 N normal force was applied to the sample, and a steady-state shear rate of 0.5 $s^{-1}$ was applied. The normal force and torque were measured for an hour. The data for a 2.5 min interval was analyzed and reported.

*Robustness Against Flow*: The apparatus shown in Figure 2b was assembled by connecting 3/4″ ID tubing to a peristaltic pump (Cole Parmer Masterflex L/S). A section of coated tubing was connected on the outlet side of the pump, and a clamp was placed downstream to adjust the outlet pressure. A flow rate of 1.5 L $min^{-1}$ was set, and at every time point, a 2 cm section of the coated tubing was removed for analysis. The contact angle was measured via the sessile drop method, in which a 3 µL drop of water was placed on the surface, imaged using a high-resolution camera and back illumination, and the angle was measured using ImageJ (NIH). The hydrogel thickness was measured by cross-sectioning the tubing, contacting it with a fluorescein solution (hydrophilic dye) and imaging it with a fluorescent microscope (Eclipse LV100ND, Nikon). The coating thickness was quantified using built-in tools (NIS-Elements software).

*Bacterial Adhesion*: An engineered *E. coli* strain that expresses green fluorescent protein (GFP) used in previous publications[47,48] was cultured in Luria-Bertani broth (LB broth) overnight at 37 °C. A 1 mL aliquot of bacteria culture was diluted in 10 mL of fresh LB broth and placed on top of flat samples (1 cm × 1 cm) and incubated for 4 h at 37 °C (static condition). For the flow condition, a scaled-down version of the apparatus in Figure 2b was set up using a VWR peristaltic pump and 3/8″ ID tubing—the bacterial solution flowed through the tubing for 8 h at 37 °C. After the incubation, the samples were taken out, gently rinsed twice with phosphate buffered saline (PBS) to remove the free-floating bacteria, and imaged with a fluorescence microscope (Eclipse LV100ND, Nikon). The bacterial coverage on the samples was quantified using Image J.

*Fibrin Deposition*: Following previously published protocols,[31,32] the wells of a 24-well plate (Corning) were blocked with 1 wt% bovine serum albumin (BSA) in PBS for 30 min and rinsed with PBS. Pristine and coated flat samples (1 × 1 cm) were placed in the blocked wells with heparinized whole human blood (0.25 U $mL^{-1}$ to prevent overall clotting) spiked with fluorescently labeled fibrinogen (Alexa Fluor 488 conjugated human fibrinogen, ThermoFischer Scientific). The samples were incubated for increasing time points on an orbital shaker at room temperature. After removing them from the well, the samples were gently rinsed with normal saline (0.9% sodium chloride) and fixed for 1 h with 2.5% glutaraldehyde in 0.1 M phosphate buffer before imaging with an upright confocal microscope (SP8, Leica). The images were analyzed and quantified with ImageJ.

*Blood Hemolysis*: Citrated bovine blood samples (≈3 mL) were placed on the inner lumen of pristine and coated tubing (3/8″ ID) for 5 min under gentle agitation. Two controls were used—as-received blood and lysed blood (20% DI water added). The blood was then poured on Eppendorf tubes and centrifuged for 2 min (VWR minicentrifuge). The supernatant was placed in disposable cuvettes and analyzed using a UV–vis spectrophotometer (BioMate 3S, Thermo Scientific) at two wavelengths, 540 and 576 nm, which correspond to the max. absorbance for oxygenated hemoglobin.

*Optical Thromboelastography*: The equipment used for these experiments was custom-built by researchers in the Nadkarni group, as described elsewhere.[51–53] The data collection and analysis algorithms are also described in those publications. Citrated human blood was placed

inside pristine and coated tubing (3/8″ ID) for 3 min, then recalcified with 0.2 M calcium chloride solution in saline (60 μL $mL^{-1}$ blood). An ≈100 μL aliquot of blood was placed in a silicone blood collection cartridge and analyzed at 37 °C until coagulation was measured. Control samples were done in which the blood was recalcified and analyzed without contacting any tubing. The parameters were obtained by fitting the OTEG curves using custom-built MATLAB algorithms.

*Blood Flow Inside Tubing Tests*: Two different types of tests were carried out. For the first type, 3 mL citrated bovine blood was recalcified using 0.5 M calcium chloride in saline (24 μL per mL blood) and placed inside pristine and coated tubing (≈9′ long, 3/8″ ID). The tubing had been previously sterilized with ethanol and UV radiation, and thoroughly rinsed with saline solution. The tubing was agitated back and forth as shown in the videos (in the Supporting Information) until a clot was formed or 25 min elapsed. The clotting time, which was determined when the blood column stopped moving, was recorded. For the second type of tests, the blood agitation was provided by a CBP roller pump (Cobe Century). Here, 20″ sections of 3/8″ ID pristine and coated tubing was filled with recalcified blood (≈25 mL) and closed into a loop by attaching a small section of 3/4″ tubing to the ends. The tubing was weighted before and after filling with blood. A 0.25 L $min^{-1}$ flow was set up until a control sample (left in Eppendorf tube) clotted. The loop contents were poured into a petri dish, the clot was placed in a weigh boat and weighted. The tubing was gently rinsed with normal saline and weighted.

*Protocols and Approvals*: The bacterial adhesion studies were approved by MIT's Committee on Assessment of Biohazards and Embryonic Stem Cell Research Oversight, and carried out in the appropriate BL-2 facilities. The human blood studies were covered under an approved protocol by the institutional review board (IRB) of the Massachusetts General Hospital (MGH), and carried out at the appropriate BL-2 facilities.

*In Vivo Device Occlusion*: The study was carried out at a research animal surgical suite at Tongji Hospital. Three female Guanxi Ba-ma pigs (28–30 kg) aged 6 months and weighing 21–22 kg, were purchased from of Hubei Yizhicheng Biotechnology Co., Ltd, China. All in vivo animal procedures follow the "Regulations of Hubei Province on the administration of experimental animals," and were reviewed and approved by "The Charter of Laboratory Animal Ethics Committee of Huazhong University of Science and Technology."

Ketamine (6–8 mg $kg^{-1}$) was injected into the gluteus maximus to induce anesthesia. An indwelling needle was placed in the ear vein, IV propofol 2 mL and fentanyl 2 mL were injected, followed by infusion of normal saline and atropine to maintain anesthesia. An endotracheal tube was placed and connected to a ventilator to supply oxygen and isoflurane. After routine disinfection of the surgical area, an incision was made, the abdominal wall, subcutaneous tissue and fascia were cut, and the femoral artery and femoral vein carefully separated upward to expose the common iliac artery and the iliac vein. The diameter of the iliac artery was ≈3 mm, and that of the iliac vein was ≈8 mm. An ≈8 cm section of the iliac artery was carefully separated and exposed. The proximal end was clamped with an arterial clamp and the distal end was clamped with a small curved hemostat. Then, a V-shaped incision was made with ophthalmic scissors 1 cm away from the clamps.

The sterilized pristine and coated devices were lubricated with saline solution, vented, and carefully inserted in the incisions of the iliac artery. The incisions were then carefully closed to avoid blood leaks. The distal hemostat was then released. Enough saline was added the groin area to fully submerge the devices, and a gauze was placed under them for ultrasound monitoring. Once the ultrasound probe was positioned correctly, the proximal clamp was released and a timer was started. Blood flow and velocity were monitored by Doppler ultrasound. The experiment was stopped once the Doppler velocity dropped to zero, indicating the formation of a clot inside the device (and complete occlusion of the lumen). The timer was stopped.

*Statistical Analysis*: No preprocessing was done for the data, and it was all analyzed using built-in functions with Microsoft Excel. For all the figures in this article, the error bars represent the SD of the set unless otherwise noted. The significance level for all *t*-tests was set at alpha = 0.05, so statistically significant difference was noted if the *p*-value was below 0.05. The *p*-value is indicated in the figures directly, caption, or discussed in the text.

For the friction tests (Figure 2a), six data points were averaged per time point. For the contact angle measurements (Figure 2b), six measurements were done per data point. For the bacterial coverage characterization (Figure 2d), six microscopy images were taken for each condition and a one-tailed *t*-test was carried out for each pair of conditions (pristine vs coated).

For the fibrin network coverage (Figure 3b), three microscopy images were taken for each data point and a two-tailed *t*-test was carried out at each time point. For the lysis experiments (Figure 3d), four absorbance measurements were obtained per condition and two-tailed test were carried out comparing the tubing conditions (pristine and coated) versus the control. For the OTEG results (Figure 3f), the parameters from six experiments normalized by the control for each experiment were analyzed and shows as a boxplot (plotted with Origin Pro. 8.5). Here the error bars (whiskers) refer to the 5th and the 95th quantile, respectively. A two-sided *t*-test was done comparing the two conditions for each OTEG parameter.

For the clotting and adhesion in vitro experiment (Figure 4c), results from three tests were used and a two-tailed *t*-test was done for each metric. For the occlusion in vivo experiment, the times measured from three experiments were used and a two-tailed was done between the coated and pristine tubing.

## Supporting Information

Supporting Information is available from the Wiley Online Library or from the author.

## Acknowledgements

The authors gratefully acknowledge all coauthors at the MGH and Tongji hospital for their valuable assistance and skills. This work was supported by the NSF (CMMI-1661627) and the Office of Naval Research (N00014-17-1-2920) and the U.S. Army Research Office through the Institute for Soldier Nanotechnologies at Massachusetts Institute of Technology (W911NF-13-D-0001).

## Conflict of Interest

The authors declare no conflict of interest.

## Author Contributions

G.P., Y.Y. and C.N. contributed equally to this work. G.P., Y.Y., C.N., and Z.H. conceived and designed the experiments. G.P. and Y.Y. fabricated the coated devices and carried out most in vitro experiments. D.T. and S.N. enabled the OTEG coagulation studies. W.R. and S.L. assisted with the in vitro blood loop studies. Q.L., Y.Z., J.W., and L.L. carried out the in vivo experiments.

## Keywords

antifouling hydrogels, antithrombotic hydrogels, hydrogel-based medical devices, tough hydrogel devices

Received: July 1, 2020
Revised: August 21, 2020
Published online:

[1] D. J. Kuter, *Oncologist* **2004**, *9*, 207.

[2] D. G. Maki, D. M. Kluger, C. J. Crnich, *Mayo Clin. Proc.* **2006**, *81*, 1159.
[3] I. H. Jaffer, J. C. Fredenburgh, J. Hirsh, J. I. Weitz, *J. Thromb. Haemostasis* **2015**, *13*, S72.
[4] S. C. Günther, C. Schwebel, R. Hamidfar-Roy, A. Bonadona, M. Lugosi, C. Ara-Somohano, C. Minet, L. Potton, J.-C. Cartier, A. Vésin, M. Chautemps, L. Styfalova, S. Ruckly, J.-F. Timsit, *Intensive Care Med.* **2016**, *42*, 1753.
[5] C. Wall, J. Moore, J. Thachil, *J. Intensive Care Soc.* **2016**, *17*, 160.
[6] K. S. Lavery, C. Rhodes, A. Mcgraw, M. J. Eppihimer, *Adv. Drug Delivery Rev.* **2017**, *112*, 2.
[7] A. Wallace, H. Albadawi, N. Patel, A. Khademhosseini, Y. S. Zhang, S. Naidu, G. Knuttinen, R. Oklu, *Cardiovasc. Diagn. Ther.* **2017**, *7*, S246.
[8] D. Grau, B. Clarivet, A. Lotthé, S. Bommart, S. Parer, *Antimicrob. Resist. Infect. Control* **2017**, *6*, 18.
[9] L. N. Tchouta, P. N. Bonde, *ASAIO J.* **2015**, *61*, 623.
[10] V. Semak, M. B. Fischer, V. Weber, *Int. J. Artif. Organs* **2017**, *40*, 22.
[11] M. Elder, *Global Market for Catheters*, BCC Research, Wellesley, MA **2016**.
[12] *The Global Market for Medical Devices*, Kalorama Information, Arlington, VA **2017**.
[13] J. S. Vanepps, J. G. Younger, *Shock* **2016**, *46*, 597.
[14] P. Parás-Bravo, M. Paz-Zulueta, R. Sarabia-Lavin, F. Jose Amo-Setién, M. Herrero-Montes, E. Olavarría-Beivíde, M. Rodríguez-Rodríguez, B. Torres-Manrique, C. Rodríguez-De La Vega, V. Caso-Álvarez, L. González-Parralo, F. M. Antolín-Juárez, *PLoS One* **2016**, *11*, e0162479.
[15] B. D. Ratner, *Biomaterials* **2007**, *28*, 5144.
[16] B. D. Ratner, *J. Biomater. Sci., Polym. Ed.* **2012**, *11*, 1107.
[17] T. M. Maul, M. P. Massicotte, P. D. Wearden, in *Extracorporeal Membrane Oxygenation - Advances in therapy* (Ed: M.S. Firstenberg), IntechOpen, **2016**, chp. 3.
[18] S. M. Hastings, D. N. Ku, S. Wagoner, K. O. Maher, S. Deshpande, *ASAIO J.* **2017**, *63*, 86.
[19] L. Lucchi, G. Ligabue, M. Marietta, A. Delnevo, M. Malagoli, S. Perrone, L. Stipo, F. Grandi, A. Albertazzi, *Artif. Organs* **2006**, *30*, 106.
[20] K. P. Sathe, W.-S. Yeo, I. D. Liu, S. Ekambaram, M. Azar, H.-K. Yap, K.-H. Ng, *BMC Nephrol.* **2015**, *16*, 3.
[21] K. B. Quencer, R. Oklu, *Cardiovasc. Diagn. Ther.* **2017**, *7*, S299.
[22] V. Tchantchaleishvili, F. Sagebin, R. E. Ross, W. Hallinan, K. Q. Schwarz, H. T. Massey, *Ann. Cardiothorac. Surg.* **2014**, *3*, 490.
[23] N. M. Lai, N. Chaiyakunapruk, N. A. Lai, E. O'Riordan, W. S. Pau, S. Saint, *Cochrane Database Syst. Rev.* **2016**, *3*, CD007878.
[24] J.-F. Timsit, Y. Dubois, C. Minet, A. Bonadona, M. Lugosi, C. Ara-Somohano, R. Hamidfar-Roy, C. Schwebel, *Ann. Intensive Care* **2011**, *1*, 34.
[25] K. G. Neoh, M. Li, E.-T. Kang, E. Chiong, P. A. Tambyah, *J. Mater. Chem. B* **2017**, *5*, 2045.
[26] X. Hou, Y. Hu, A. Grinthal, M. Khan, J. Aizenberg, *Nature* **2015**, *519*, 70.
[27] I. Sotiri, A. Tajik, Y. Lai, C. T. Zhang, Y. Kovalenko, C. R. Nemr, H. Ledoux, J. Alvarenga, E. Johnson, H. S. Patanwala, J. V. I. Timonen, Y. Hu, J. Aizenberg, C. Howell, *Biointerphases* **2018**, *13*, 06D401.
[28] D. Zhang, Z. Xu, H. Li, C. Fan, C. Cui, T. Wu, M. Xiao, Y. Yang, J. Yang, W. Liu, *Biomater. Sci.* **2020**, *8*, 1455.
[29] P. W. Heyman, C. S. Cho, J. C. Mcrea, D. B. Olsen, S. W. Kim, *J. Biomed. Mater. Res.* **1985**, *19*, 419.
[30] R. Biran, D. Pond, *Adv. Drug Delivery Rev.* **2017**, *112*, 12.
[31] M. F. Maitz, J. Zitzmann, J. Hanke, C. Renneberg, M. V. Tsurkan, C. Sperling, U. Freudenberg, C. Werner, *Biomaterials* **2017**, *135*, 53.
[32] I. Reviakine, F. Jung, S. Braune, J. L. Brash, R. Latour, M. Gorbet, W. Van Oeveren, *Blood Rev.* **2017**, *31*, 11.
[33] T.-S. Wong, S. H. Kang, S. K. Y. Tang, E. J. Smythe, B. D. Hatton, A. Grinthal, J. Aizenberg, *Nature* **2011**, *477*, 443.
[34] A. K. Epstein, T.-S. Wong, R. A. Belisle, E. M. Boggs, J. Aizenberg, *Proc. Natl. Acad. Sci. USA* **2012**, *109*, 13182.
[35] D. C. Leslie, A. Waterhouse, J. B. Berthet, T. M. Valentin, A. L. Watters, A. Jain, P. Kim, B. D. Hatton, A. Nedder, K. Donovan, E. H. Super, C. Howell, C. P. Johnson, T. L. Vu, D. E. Bolgen, S. Rifai, A. R. Hansen, M. Aizenberg, M. Super, J. Aizenberg, D. E. Ingber, *Nat. Biotechnol.* **2014**, *32*, 1134.
[36] L. Faxälv, T. Ekblad, B.o Liedberg, T. L. Lindahl, *Acta Biomater.* **2010**, *6*, 2599.
[37] T. Ekblad, L. Faxälv, O. Andersson, N. Wallmark, A. Larsson, T. L. Lindahl, B. Liedberg, *Adv. Funct. Mater.* **2010**, *20*, 2396.
[38] M. Baghai, N. Tamura, F. Beyersdorf, M. Henze, O. Prucker, J. Rühe, S. Goto, B. Zieger, C. Heilmann, *ASAIO J.* **2014**, *60*, 587.
[39] Z. K. Zander, M. L. Becker, *ACS Macro Lett.* **2017**, *7*, 16.
[40] H. S. Nanda, A. H. Shah, G. Wicaksono, O. Pokholenko, F. Gao, I. Djordjevic, T. W. J. Steele, *Biomacromolecules* **2018**, *19*, 1425.
[41] US Food & Drug Administration, Lubricious Coating Separation from Intravascular Medical Devices: FDA Safety Communication **2015**, safety communication, https://www.fda.gov/media/113951/download (accessed: August 2020).
[42] R. I. Mehta, R. I. Mehta, *Am. J. Med.* **2017**, *130*, e287.
[43] A. M. Chopra, M. Mehta, J. Bismuth, M. Shapiro, M. C. Fishbein, A. G. Bridges, H. V. Vinters, *Cardiovasc. Pathol.* **2017**, *30*, 45.
[44] L. Chen, D. Han, L. Jiang, *Colloids Surf., B* **2011**, *85*, 2.
[45] US Food & Drug Administration, Intravascular Catheters, Wires, and Delivery Systems with Lubricious Coatings—Labeling Considerations: FDA Guidance **2019**, guidance, https://www.fda.gov/media/113951/download (accessed: August 2020).
[46] H. Yuk, T. Zhang, G. A. Parada, X. Liu, X. Zhao, *Nat. Commun.* **2016**, *7*, 12028.
[47] G. A. Parada, H. Yuk, X. Liu, A. J. Hsieh, X. Zhao, *Adv. Healthcare Mater.* **2017**, *6*, 1700520.
[48] Y. Yu, H. Yuk, G. A. Parada, Y. Wu, X. Liu, C. S. Nabzdyk, K. Youcef-Toumi, J. Zang, X. Zhao, *Adv. Mater.* **2019**, *31*, 1807101.
[49] J. Sakamoto, K. Hashimoto, *Arch. Toxicol.* **1985**, *57*, 282.
[50] Z. He, C. Wu, M. Hua, S. Wu, D. Wu, X. Zhu, J. Wang, X. He, *Matter* **2020**, *2*, 723.
[51] D. Kaneko, T. Tada, T. Kurokawa, J. P. Gong, Y. Osada, *Adv. Mater.* **2005**, *17*, 535.
[52] J. P. Gong, Y. Katsuyama, T. Kurokawa, Y. Osada, *Adv. Mater.* **2003**, *15*, 1155.
[53] X. Dai, Y. Zhang, L. Gao, T. Bai, W. Wang, Y. Cui, W. Liu, *Adv. Mater.* **2015**, *27*, 3566.
[54] I. Eshet, V. Freger, R. Kasher, M. Herzberg, J. Lei, M. Ulbricht, *Biomacromolecules* **2011**, *12*, 2681.
[55] ISO, German Institute for Standardization, Berlin, Germany *Biological Evaluation of Medical Devices—Part 4: Selection of Tests for Interactions with Blood*, British Standards Institution (BSI), London **2017**.
[56] L.-C. Xu, J. W. Bauer, C. A. Siedlecki, *Colloids Surf., B* **2014**, *124*, 49.
[57] E. J. van Kampen, W. G. Zijlstra, *Adv. Clin. Chem.* **1966**, *8*, 141, https://www.fda.gov/media/113951/download.
[58] M. M. Tripathi, Z. Hajjarian, E. M. Van Cott, S. K. Nadkarni, *Biomed. Opt. Express* **2014**, *5*, 817.
[59] M. M. Tripathi, S. Egawa, A. G. Wirth, D. M. Tshikudi, E. M. Van Cott, S. K. Nadkarni, *Sci. Rep.* **2017**, *7*, 9169, https://www.fda.gov/media/113951/download.
[60] D. M. Tshikudi, M. M. Tripathi, Z. Hajjarian, E. M. Van Cott, S. K. Nadkarni, *PLoS One* **2017**, *12*, e0182491.

 